Makara Journal of Science

Volume 28
Issue 3 *September*

Article 9

9-25-2024

Cellular Uptake and Computational Analysis of [131I]-Xanthine and [131I]-Hypoxanthine in Human Prostate Cancer Cell Line (LNCaP)

Hendris Wongso
Research Center for Radioisotope, Radiopharmaceutical, and Biodosimetry Technology, Research Organization for Nuclear Energy, National Research and Innovation Agency, Puspiptek, Banten 15314, Indonesia, hend042@brin.go.id

Isa Mahendra
Research Center for Radioisotope, Radiopharmaceutical, and Biodosimetry Technology, Research Organization for Nuclear Energy, National Research and Innovation Agency, Puspiptek, Banten 15314, Indonesia

Yanuar Setiadi
Research Center for Environmental and Clean Technology, Research Organization for Life Sciences and Environment, National Research and Innovation Agency, Puspiptek, Banten 15314, Indonesia

Badra Sanditya Rattyananda
Research Center for Radioisotope, Radiopharmaceutical, and Biodosimetry Technology, Research Organization for Nuclear Energy, National Research and Innovation Agency, Puspiptek, Banten 15314, Indonesia

Asep Rizaludin
Research Center for Radioisotope, Radiopharmaceutical, and Biodosimetry Technology, Research Organization for Nuclear Energy, National Research and Innovation Agency, Puspiptek, Banten 15314, Indonesia

See next page for additional authors

Recommended Citation
Wongso, Hendris; Mahendra, Isa; Setiadi, Yanuar; Rattyananda, Badra Sanditya; Rizaludin, Asep; Pranisuari, Ni Made Yuktikamura Galih; and Kusumaningrum, Crhisterra Ellen (2024) "Cellular Uptake and Computational Analysis of [131I]-Xanthine and [131I]-Hypoxanthine in Human Prostate Cancer Cell Line (LNCaP)," *Makara Journal of Science*: Vol. 28: Iss. 3, Article 9.
DOI: 10.7454/mss.v28i3.2140
Available at: https://scholarhub.ui.ac.id/science/vol28/iss3/9

Cellular Uptake and Computational Analysis of [131I]-Xanthine and [131I]-Hypoxanthine in Human Prostate Cancer Cell Line (LNCaP)

Authors

Hendris Wongso, Isa Mahendra, Yanuar Setiadi, Badra Sanditya Rattyananda, Asep Rizaludin, Ni Made Yuktikamura Galih Pranisuari, and Crhisterra Ellen Kusumaningrum

Makara Journal of Science, 28/3 (2024), 257-263
doi: 10.7454/mss.v28i3.2140

Cellular Uptake and Computational Analysis of [^{131}I]-Xanthine and [^{131}I]-Hypoxanthine in Human Prostate Cancer Cell Line (LNCaP)

Hendris Wongso[1,2*], Isa Mahendra[1,2], Yanuar Setiadi[3], Badra Sanditya Rattyananda[1], Asep Rizaludin[1], Ni Made Yuktikamura Galih Pranisuari[1,4], and Crhisterra Ellen Kusumaningrum[1]

1. Research Center for Radioisotope, Radiopharmaceutical, and Biodosimetry Technology, Research Organization for Nuclear Energy, National Research and Innovation Agency, Puspiptek, Banten 15314, Indonesia
2. Research Collaboration Center for Theranostic Radiopharmaceuticals, National Research and Innovation Agency, Jatinangor 45363, Indonesia
3. Research Center for Environmental and Clean Technology, Research Organization for Life Sciences and Environment, National Research and Innovation Agency, Puspiptek, Banten 15314, Indonesia
4. Indonesian Nuclear Technology Polytechnic, Sleman, Yogyakarta 55281, Indonesia

E-mail: hend042@brin.go.id

Received July 14, 2023 | Accepted August 5, 2024

Abstract

Potent radiolabelled compounds eligible for therapy of prostate cancer need to be developed. Hence, we developed two candidate therapeutic agents bearing the iodine-131 (^{131}I) radionuclide, namely, [^{131}I]-xanthine (3,7-dihydropurine-2,6-dione) and [^{131}I]-hypoxanthine (1,9-dihydro-6*H*-purin-6-one). The radiolabelled compounds were subjected to a cellular uptake study, which was accomplished by incubating [^{131}I]-xanthine and [^{131}I]-hypoxanthine with the human prostate cancer cell line (LNCaP) for 5, 15, 30, 60, and 90 min. Results showed that the accumulation of both [^{131}I]-xanthine and [^{131}I]-hypoxanthine in prostate cancer cells was significantly higher than the control group (^{131}I). [^{131}I]-xanthine rapidly accumulated in prostate cancer cells, with the highest percentage of cellular uptake of 2.73% ± 0.40% observed at 30 min of incubation. By contrast, [^{131}I]-hypoxanthine exhibited more efficient accumulation in prostate cancer cells, especially at 60 and 90 min of incubation, with cellular uptake values of 11.5% ± 3.14% and 11.9% ± 1.83%, respectively. Furthermore, the computational analysis showed that radioiodinated xanthine and hypoxanthine provide potential binding affinities and interaction on both androgen and prostate-specific membrane antigen receptors. Overall, this study indicates that [^{131}I]-xanthine and [^{131}I]-hypoxanthine can be potentially developed as therapeutic agents for prostate cancer.

Keywords: cellular uptake, computational analysis, prostate cancer, [^{131}I]-hypoxanthine, [^{131}I]-xanthine

Introduction

Prostate cancer is the second most frequently diagnosed malignancy and the sixth leading cause of death in men worldwide in 2021, which has become a global health concern [1, 2]. A previous study proposed that the pathogenesis of prostate cancer is driven by the androgen receptor (a ligand-dependent transcription factor from the nuclear receptor family) [3]. The standard of care for therapy often includes the use of novel drugs [3], hormonal therapy [4], and radiotherapy [5]. Over the past decade, tremendous technological improvements in biomedical science have been made. In particular, the advancement in the treatment of prostate cancer using prostate-specific membrane antigen (PSMA) radioligand therapy has positively contributed to the overall patient outcome in clinical settings [5, 6].

β-Emitting radionuclides have been widely reported to deliver therapeutic radiation to prostate cancer cells. Of *β*-emitting radionuclides, lutetium-177 (^{177}Lu), yttrium-90 (^{90}Y), terbium-161 (^{161}Tb), and iodine-131 (^{131}I) have been utilized for the immunotherapy-based treatment of prostate cancer [7]. ^{131}I ($t_{1/2}$ = 8.02 days, E_{β} = 0.607 MeV) is one of the most commonly used *β*-emitter radionuclides in nuclear medicine for the therapeutic purposes of several diseases, including thyroid cancer, neuroblastoma, and pheochromocytoma. ^{131}I can be directly conjugated with a phenol group on active material by simple oxidation, followed by an electrophilic substitution reac-

tion using an oxidizing agent (e.g., iodogen and chloramine-T) [8]. Moreover, a radioiodine atom can be attached to the side chain of the molecule bearing the imidazole group [9].

Oxidative stress, a relative excess of reactive oxygen species, is a hallmark of cancer and has been linked with the progression and pathogenesis of prostate cancer, especially in therapeutic resistance and tumor metastasis [10, 11]. A previous study proposed that human xanthine oxidoreductase plays an important role in the process of oncogenesis by directly catalyzing the metabolic activation of carcinogenic substances or indirectly by producing reactive oxygen and nitrogen species [12]. Veljkovic *et al.* investigated whether xanthine oxidase/ dehydrogenase activity is the origin of oxidative stress in prostate tissue and determined that the activity of xanthine oxidase was significantly higher in tumors than in healthy tissue. Thus, xanthine oxidase could be a promising theranostic biomarker of cancers, especially prostate cancer [10].

Xanthine (3,7-dihydropurine-2,6-dione) and hypoxanthine (1,9-dihydro-6*H*-purin-6-one) are purine-based compounds (alkaloids) found in nearly all living species, such as plants, animals, and human body tissues [13, 14]. In particular, xanthine has been used in many studies as a lead compound for the synthesis of a wide variety of pharmacologically active molecules, such as aminophylline, pentoxifylline, propentofylline, doxofylline, and others. Furthermore, several compounds bearing the xanthine scaffold, such as caffeine, theophylline, theobromine, and paraxanthine, exhibit a broad range of biological activities and, therefore, have been used as important pharmacophores in drug development (Figure 1) [15].

In our previous study, the radiosynthesis of [^{131}I]-xanthine and [^{131}I]-hypoxanthine was successfully achieved [16]. Here, we report the computational analysis of these radiolabelled purine-based compounds on androgen and PMSA receptors. Moreover, the capability of the radiolabelled compounds to recognize prostate cancer was measured by a cellular uptake study in the human prostate cancer cell line (LNCaP).

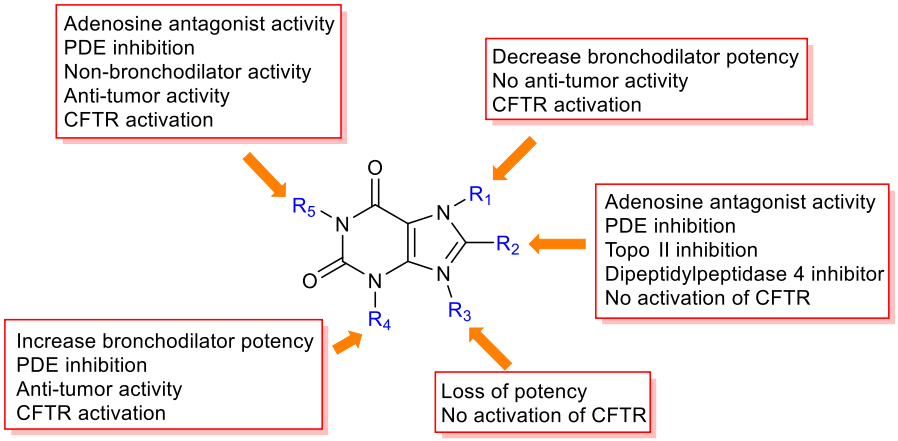

Figure 1. Potential Modification Sites of the Xanthine Scaffold to Generate Specific Pharmacological Activities [15]

Materials and Methods

Materials and instruments. Unless stated otherwise, all laboratory-grade or reagent-grade chemicals were purchased from Merck Singapore and were used without further purification. Radiosynthesis of [^{131}I]-xanthine and [^{131}I]-hypoxanthine was accomplished in our previous study (AIJ) and further used for in vitro study. NaI-131 solution was produced by the G.A. Siwabessy Multi-Purpose Reactor (Directorate of Nuclear Facility Management) and subsequently prepared by the researchers (Anung Pujiyanto, Daya Agung Sarwono, and team) at the Research Center for Radioisotope, Radiopharmaceutical, and Biodosimetry Technology, National Research and Innovation Agency of Indonesia (BRIN). The human prostate cancer cell line (LNCaP) clone FGC was purchased from the European Collection of Authenticated Cell Cultures (Salisbury, UK). The Roswell Park Memorial Institute 1640 medium (RPMI 1640; American Type Culture Collection modification) was purchased from Gibco (Paisley, UK). Fetal bovine serum (FBS), sodium pyruvate, and penicillin–streptomycin antibiotic were purchased from Sigma-Aldrich (Saint Louis, MO, USA). Avogadro, ORCA, AutoDockTools 1.5.6, AutoDock Vina, and BIOVIA Discovery Studio (freeware) and Amber 18 (licensed) were employed for computational simulations.

Cell culture. The human prostate cancer cell line (LNCaP) was grown in RPMI 1640 medium supplemented with 1.0 mM sodium pyruvate, 10% FBS, and 1.0% penicillin–streptomycin antibiotic (penicillin = 100 IU/mL and streptomycin = 100 mg/mL) at 37 °C in

5% CO_2 atmosphere. The cell was harvested with 0.25% trypsin/EDTA and centrifuged at 100g for 7 min.

Cellular uptake. The human prostate cancer cell line (LNCaP; 2.0 × 10^5 cells/well) was cultured in 24-well culture plates in a complete medium and incubated overnight. The medium was discarded, and the cells were rinsed with Hank's balanced salt solution (HBSS). Subsequently, [^{131}I]-hypoxanthine, [^{131}I]-xanthine, and NaI-131 (0.7 MBq in 10 µL solution) were added to each well containing HBSS and incubated at 37 °C for 5, 15, 30, 60, and 90 min. Then, the cells were washed with HBSS and lysed using a sodium hydroxide solution (0.1 M). The cell lysates were counted using a Wizard2® 2470 automatic gamma counter (PerkinElmer, Waltham, MA, USA) to determine the radioactivity. The results of cellular uptake were expressed as the percentage of cellular uptake determined using the following formula:

$$\%\ Uptake = \frac{Count\ value\ of\ cell\ lysates}{Count\ value\ of\ a\ 0.7\ MBq\ of\ \ radiolabeled\ compound}\ x\ 100\%.$$

Computational analysis. Xanthine, hypoxanthine, [^{131}I]-xanthine, and [^{131}I]-hypoxanthine structures were drawn using the Avogadro software and optimized using ORCA 5.03 with the B3LYP functional and DEF2-SVP basis set. The structures were docked with AutoDock Vina 1.23 on the binding pocket of receptors, which were predominantly detected in prostate cancer cells, thus representing the most suitable receptors to achieve the main purpose of our study. Receptor structures were obtained from the RCSB Protein Data Bank (androgen receptor—PDB ID: 2AM9, PSMA-PDB ID: 5O5T) and were extracted by removing the ligands. Best conformations from docking simulations were used for molecular dynamics (MD) simulations using Amber 18. The MD simulations were performed for 100 ns at 37 °C and 1 atm.

Statistical analysis. The results of radiochemical purity and cellular uptake were expressed as a percentage of the mean ± SD. The differences among multiple groups in the cellular uptake study were analyzed via a one-way analysis of variance. Differences were considered significant when the p value was <0.05. The statistical analyses were performed using GraphPad Prism software version 8.4.3 (686) (GraphPad Software, La Jolla, CA, USA).

Results and Discussion

In our previous study, we successfully radiolabelled xanthine and hypoxanthine with ^{131}I (Figure 2) under mild reaction conditions to produce [^{131}I]-xanthine and [^{131}I]-hypoxanthine with moderate radiochemical yield and high radiochemical purity [16]. The current study presents a preliminary evaluation of these radioiodinated purine-based molecules for their potential application in the therapy of prostate cancer.

The radioiodinated xanthine and hypoxanthine are categorized as small molecules with molecular weight of <1 kDa. Cellular uptake studies indicate that both [^{131}I]-xanthine and [^{131}I]-hypoxanthine can penetrate prostate cancer cells in a time-dependent manner (Figure 3). Overall, the results showed that the accumulation of radioiodinated xanthine and hypoxanthine in prostate cancer cells was significantly higher than in the control group (^{131}I). [^{131}I]-xanthine rapidly accumulated in prostate cancer cells, with the highest percentage of cellular uptake of 2.73% ± 0.40% observed at 30 min of incubation, which was sevenfold higher than in the control group. However, the accumulation was slightly decreased to 2.59% ± 0.30% and 1.68% ± 0.27% after 60 and 90 min of incubation, respectively.

By contrast, [^{131}I]-hypoxanthine exhibited more efficient internalization in prostate cancer cells, especially at 60 and 90 min of incubation, with cellular uptake values of 11.5% ± 3.14% and 11.9% ± 1.83%, respectively, or approximately 88-fold and 170-fold higher than in the control group, respectively. The uptake values of [^{131}I]-hypoxanthine at 5 min (1.10% ± 0.99%), 15 min (1.09% ± 0.78%), and 30 min (1.34% ± 0.29%) of incubation were slightly lower than those of [^{131}I]-xanthine; however, [^{131}I]-hypoxanthine exhibited fourfold and sevenfold higher accumulation in prostate cancer cells at 30 and 90 min of incubation, respectively.

Generally, the majority of small drugs, including [^{131}I]-xanthine and [^{131}I]-hypoxanthine, penetrate cells through simple diffusion, which requires that they are at least slightly soluble in the lipid bilayer component of cell membranes [17]. By contrast, several hydrophilic small active compounds showed insufficient bioavailability because of poor membrane permeability [18]. Hence, in some circumstances, the penetration of drugs into the cells is regulated by other mechanisms, such as transporter, channel, and receptor [19]. Xanthine and hypoxanthine are considered hydrophilic molecules. The introduction of halogen (e.g., iodine) to the molecules increases hydrophobicity [20−22] and may be the reason for the considerably high cellular uptake values in prostate cancer cells.

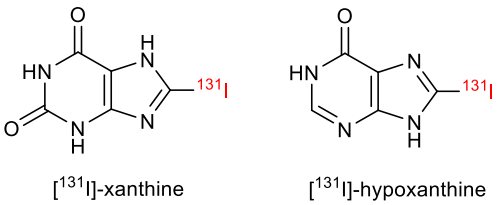

Figure 2. Plausible Structures of [^{131}I]-xanthine and [^{131}I]-hypoxanthine [16]

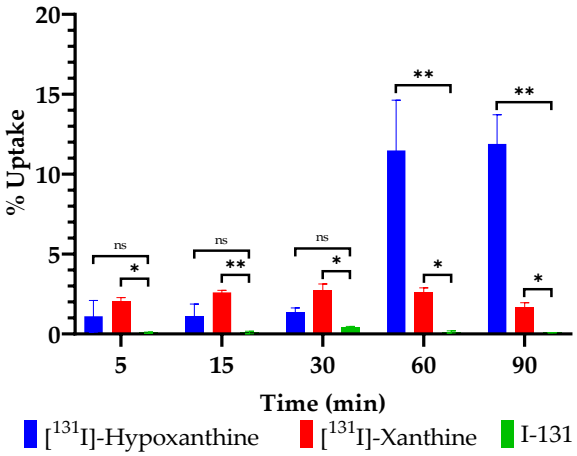

Figure 3. Cellular Uptake of [^{131}I]-xanthine, [^{131}I]-hypoxanthine, and Iodine-131 (control) in the Human Prostate Cancer Cell Line (LNCaP); *p < 0.05, **p < 0.01

Table 1. Docking scores of the tested compounds on androgen and prostate-specific membrane antigen (PSMA) receptors

Compound Name	Androgen Receptor		PSMA Receptor	
	Binding Affinity (kcal/mol)	Interactions	Binding Affinity (kcal/mol)	Interactions
Xanthine	−5.8	Gly708, Met745, Arg752, Met787 (H-bond)	−6.4	Gly206, Val208, Gly548 (H-bond) Lys207, Gln254, Tyr700 (hydrophobic interactions)
[^{131}I]-xanthine	−6.1	Gly708, Met745, Arg752, Met787 (H-bond) Leu704, Met749, Phe764 (hydrophobic interactions)	−7.0	Gly206, Val208, Gly548 (H-bond) Lys207, Gln254, Phe546, Tyr552, Tyr700 (hydrophobic interactions)
Hypoxanthine	−5.4	Met745 (H-bond)	−6.0	Val208, Tyr234, Gly548 (H-bond) Tyr552 (hydrophobic interactions)
[^{131}I]-hypoxanthine	−5.8	Met745 (H-bond) Met742, Met741 (hydrophobic interactions)	−6.5	Val208, Tyr234, Gly548 (H-bond) Tyr552, Trp541, Phe546, Tyr700 (hydrophobic interactions)

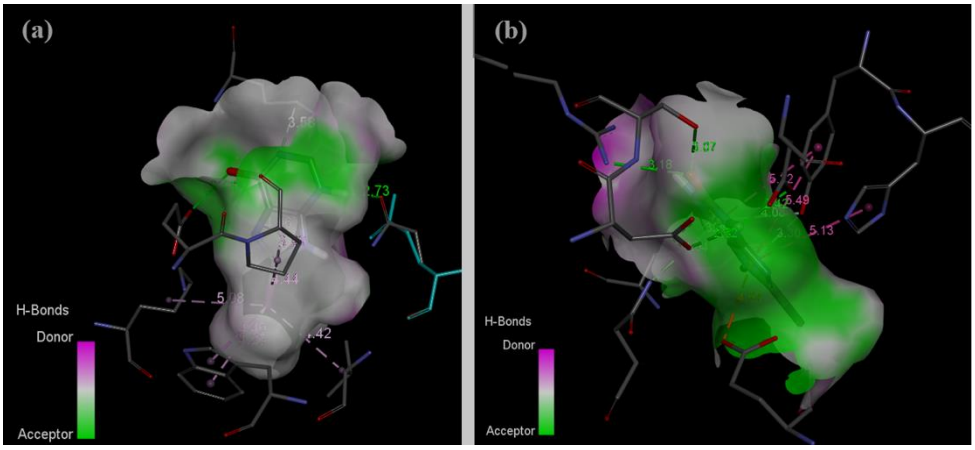

Figure 4. Maps of the Donor and Acceptor of the Hydrogen Bond of the Androgen (a) and Prostate-Specific Membrane Antigen (PSMA) (b) Receptor Binding Pockets and Their Interaction with [^{131}I]-xanthine (The Distance Between Each Amino Acid that is Responsible for Binding is Shown)

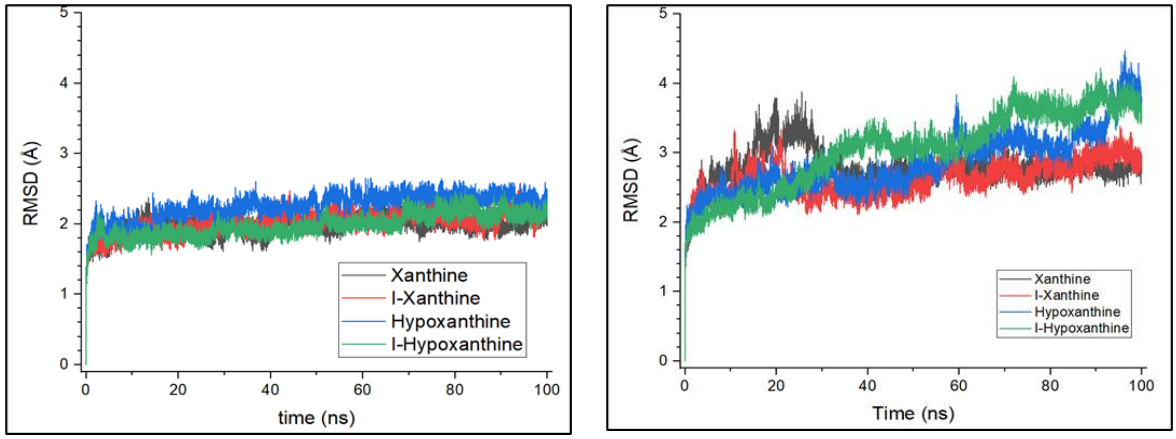

(a) (b)

Figure 5. RMSD analysis of the Compound–androgen Receptor (a) and Compound–PSMA Receptor (b) Interactions

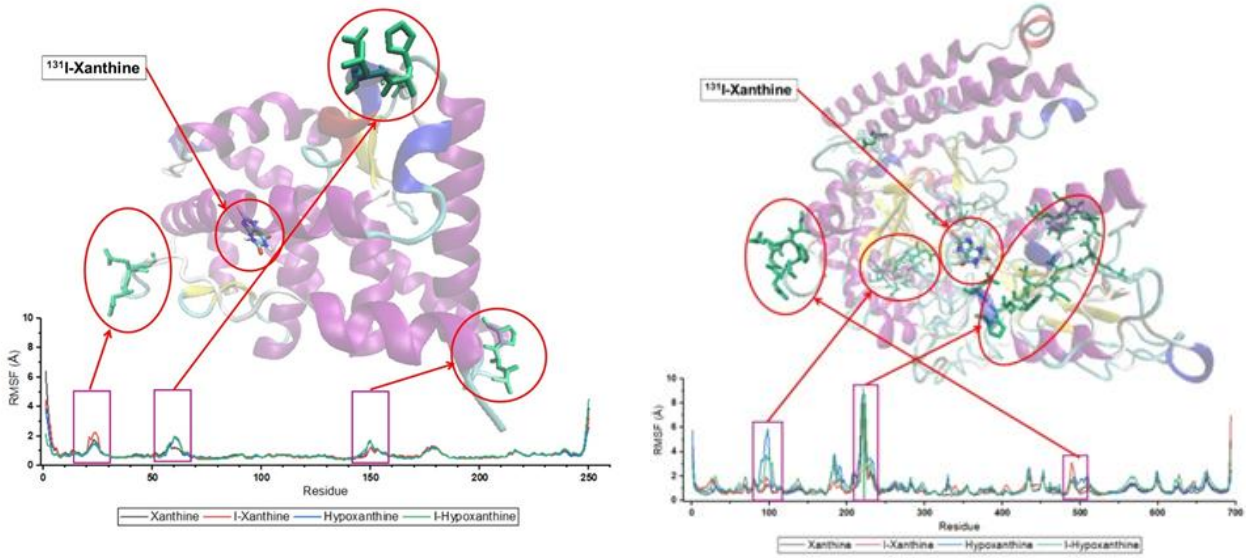

(a) (b)

Figure 6. RMSF of [^{131}I]-xanthine in the Androgen (a) and PSMA (b) Receptors

To further evaluate the potential binding of [^{131}I]-xanthine and [^{131}I]-hypoxanthine on prostate cancer cells, we performed molecular modeling studies (computational analysis) using androgen and PSMA receptors as targeted receptors. All compounds (i.e., xanthine, hypoxanthine, iodinated xanthine, and iodinated hypoxanthine) have been successfully docked with the androgen and PSMA receptors. Furthermore, the interaction of the tested compounds with several residues in androgen and PSMA receptors is described in Table 1.

Overall, the docking results indicated a good binding affinity of all tested compounds in both receptors. However, the compound–PSMA receptor interaction showed a stronger bond than the compound–androgen receptor interaction because the binding pocket on the PSMA receptor has a better tendency to form hydrogen bonds (H-bonds), as shown in the H-bond donor–acceptor maps in Figure 4. PSMA provided an H-bond donor, which is denoted by the magenta areas, and an H-bond acceptor, which is denoted by the green areas (Figure 4b), whereas the androgen receptor provided fewer interactions (Figure 4a). Furthermore, the binding energy of xanthine is lower than that of hypoxanthine on both receptors. More oxygen atoms in the xanthine structure formed H-bonds with the methionine and arginine residues on the androgen binding pocket and with the glycine residue on PSMA. The docking results also showed that iodinated compounds of xanthine and hypoxanthine have better binding affinity than their initial molecules. Iodine exhibited a hydrophobic interaction with leucine on the [^{131}I]-xanthine–androgen receptor, tryptophane and methionine on the [^{131}I]-hypoxanthine–androgen receptor, phenylalanine on the [^{131}I]-xanthine–PSMA receptor, and phenylalanine and tryptophane on the [^{131}I]-hypoxanthine–PSMA receptor.

Furthermore, the MD simulation results of the tested compounds revealed that all compounds exhibited good stability on the androgen and PSMA receptors within the period of simulation (100 ns), as indicated by the RMSD data (Figure 5). Specifically, the RMSD results of all compounds on the androgen receptor were stable at approximately 2.2 Å. The RMSD results of the PSMA receptor with xanthine and [^{131}I]-xanthine were also stable at approximately 2.9 Å. However, hypoxanthine and [^{131}I]-hypoxanthine exhibited lower stability until 100 ns.

The RMSF graphic of [^{131}I]-xanthine in the androgen receptor showed no significant fluctuation/flexibility of residues during the MD simulation as the value of RMSF on every residue was no more than 4 Å (Figure 6a). The RMSF of [^{131}I]-xanthine in the PSMA receptor showed considerably high fluctuations near residues 220, 100, and 480. All of the highly fluctuating residues were located near the compounds (Figure 6b). Limited fluctuation was detected in residues 693, 730, 819, and 848 because of fewer H-bond interactions formed.

Conclusion

In conclusion, the cellular uptake of two radiolabelled purine-based molecules, i.e., [^{131}I]-xanthine and [^{131}I]-hypoxanthine, was significantly higher than that of the control group (^{131}I). Hence, the preliminary in vitro results indicated the potential use of these compounds as therapeutic agents for prostate cancer. The presence of ^{131}I will ensure the delivery of the radiation dose to destroy cancerous tissues. Furthermore, ^{131}I can be an ideal choice because of its exceptional physical (half-life) and therapeutic (beta energy) properties, availability, and affordability. Computational simulations of xanthine, hypoxanthine, and their iodinated derivatives exhibited good binding affinities ranging between 5 and 7 kcal/mol and good stability on the androgen and PSMA receptors.

CRediT Authorship Contribution Statement

H.W. contributed as the main contributor to this paper. Conceptualization, H.W; methodology, H.W, I.M, Y.S, and B.S.R; software, H.W, Y.S, and B.S.R; investigation, H.W, I.M, Y.S, B.S.R, N.M.Y.G.P, and C.E.K; writing—original draft preparation, H.W, I.M, Y.S, B.S.R, and C.E.K; writing—review and editing, H.W, I.M, Y.S, B.S.R; visualization, C.E.K.; supervision, H.W. All authors have read and agreed to the published version of the manuscript.

Declaration of Competing Interest

The authors declare no competing financial interest.

Acknowledgment

We thank the colleagues at the G.A. Siwabessy Multi-Purpose Reactor, Directorate of Nuclear Facility Management, and Radioisotope Research Group (PRTRRB), National Research and Innovation Agency Republic of Indonesia for their valuable help in providing iodine-131.

References

[1] Debnath, S., Zhou, N., McLaughlin, M., Rice, S., Pillai, A.K., Hao, G., *et al*. 2022. PSMA-targeting imaging and theranostic agents-current status and future perspective. Int. J. Mol. Sci. 23(3): 1158, https://doi.org/10.3390/ijms23031158.

[2] Teoh, J.Y.C., Hirai, H.W., Ho, J.M.W., Chan, F.C.H., Tsoi, K.K.F., Ng, C.F. 2019. Global incidence of prostate cancer in developing and developed countries with changing age structures. PLoS One. 14(10): e0221775, https://doi.org/10.1371/journal.pone.0221775.

[3] Nevedomskaya, E., Baumgart, S.J., Haendler, B. 2018. Recent advances in prostate cancer treatment and drug discovery. Int. J. Mol. Sci. 19(5): 1359, https://doi.org/10.3390/ijms19051359.

[4] Swami, U., Sinnott, J.A., Haaland, B., Sayegh, N., McFarland, T.R., Tripathi, N., *et al*. 2021. Treatment pattern and outcomes with systemic therapy in men with metastatic prostate cancer in the real-world patients in the United States. Cancers. 13(19): 4951, https://doi.org/10.3390/cancers13194951.

[5] Karagiannis, V., Wichmann, V., Saarinen, J., Eigeliene, N., Andersen, H., Jekunen, A. 2022. Radiotherapy treatment modification for prostate cancer patients based on PSMA-PET/CT. Radiat. Oncol. 17: 19, https://doi.org/10.1186/s13014-022-01989-5.

[6] Inubushi, M., Miura, H., Kuji, I., Ito, K., Minamimoto, R. 2020. Current status of radioligand therapy and positron-emission tomography with prostate-specific membrane antigen. Ann. Nucl. Med. 34: 879–883, https://doi.org/10.1007/s12149-020-01549-5.

[7] Czerwinska, M., Bilewicz, A., Kruszewski, M., Wegierek-Ciuk, A., Lankoff, A. 2020. Targeted radionuclide therapy of prostate cancer-from basic research to clinical perspectives. Molecules. 25(7): 1743, https://doi.org/10.3390/molecules25071743.

[8] Jeon J. 2019. Review of therapeutic applications of radiolabeled functional nanomaterials. Int. J. Mol. Sci. 20(9): 2323, https://doi.org/10.3390/ijms20092323.

[9] Kusumaningrum, C.E., Widyasari, E.M., Sriyani, M.E., Wongso, H. 2021. Pharmacological activities and potential use of bovine colostrum for peptide-based radiopharmaceuticals: A review. Pharmacia. 68(2): 471–477, https://doi.org/10.3897/pharmacia.68.e65537.

[10] Veljkovic, A., Hadzi-Dokic, J., Sokolovic, D., Basic, D., Velickovic-Jankovic, L., Stojanovic, M., *et al*. 2020. Xanthine oxidase/dehydrogenase activity as a source of oxidative stress in prostate cancer tissue. Diagnostics. 10(9): 668, https://doi.org/10.3390/diagnostics10090668.

[11] Hayes, J.D., Dinkova-Kostova, A.T., Tew, K.D. 2020. Oxidative stress in cancer. Cancer Cell. 38(2): 167–197, https://doi.org/10.1016/j.ccell.2020.06.001.

[12] Battelli, M.G., Polito, L., Bortolotti, M., Bolognesi, A. 2016. Xanthine oxidoreductase in cancer: More than a differentiation marker. Cancer Med. 5(3): 546–557, https://doi.org/10.1002/cam4.601.

[13] Kostić, D.A., Dimitrijević, D.S., Stojanović, G.S., Palić, I.R., Đorđević, A.S., Ickovski, J.D. 2015. Xanthine oxidase: Isolation, assays of activity, and inhibition. J. Chem. 2015(1): 294858, https://doi.org/10.1155/2015/294858.

[14] Khan, M.Z.H., Ahommed, M.S., Daizy, M. 2020. Detection of xanthine in food samples with an electrochemical biosensor based on PEDOT:PSS and functionalized gold nanoparticles. RSC Adv. 10(59): 36147–36154, https://doi.org/10.1039/d0ra06806c.

[15] Singh, N., Shreshtha, A.K., Thakur, M.S., Patra, S. 2018. Xanthine scaffold: Scope and potential in drug development. Heliyon. 4(10): e00829, https://doi.org/10.1016/j.heliyon.2018.e00829.

[16] Wongso, H., Nuraeni, W., Rosyidiah, E. 2022. Efficient and practical radiosynthesis of novel [131I]-xanthine and [131I]-hypoxanthine. Atom Indonesia. 48(3): 1–7, https://doi.org/10.17146/aij.2022.1233.

[17] Mosquera, J., Garcia, I., Liz-Marzan, L.M. 2018. Cellular uptake of nanoparticles versus small molecules: A matter of size. Acc. Chem. Res. 51(9): 2305–2313, https://doi.org/10.1021/acs.accounts.8b00292.

[18] Zhang, R., Qin, X., Kong, F., Chen, P., Pan, G. 2019. Improving cellular uptake of therapeutic entities through interaction with components of cell membrane. Drug Deliv. 26(1): 328–342, https://doi.org/10.1080/10717544.2019.1582730.

[19] Behzadi, S., Serpooshan, V., Tao, W., Hamaly, M.A., Alkawareek, M.Y., Dreaden, E.C., *et al*. 2017. Cellular uptake of nanoparticles: Journey inside the cell. Chem. Soc. Rev. 46(14): 4218–4244, https://doi.org/10.1039/c6cs00636a.

[20] Dedieu, A., Gaillard, J.C., Pourcher, T., Darrouzet, E., Armengaud, J. 2011. Revisiting iodination sites in thyroglobulin with an organ-oriented shotgun strategy. J. Biol. Chem. 286(1): 259–269, https://doi.org/10.1074/jbc.M110.159483.

[21] Gerebtzoff, G., Li-Blatter, X., Fischer, H., Frentzel, A., Seelig, A. 2004. Halogenation of drugs enhances membrane binding and permeation. ChemBioChem. 5(5): 676–684, https://doi.org/10.1002/cbic.200400017.

[22] Priimagi, A, Cavallo, G, Metrangolo, P., Resnati, G. 2013. The halogen bond in the design of functional supramolecular materials: Recent advances. Acc. Chem. Res. 46(11): 2686–2695, https://doi.org/10.1021/ar400103r.